Formation of C_mH_n ($m \geqslant 3$, $n \leqslant m$) hydrocarbons from C_1 and C_2 molecules by high-temperature ($\geqslant$1000 °C), short-contact-time (1–10 ms) nozzle beam reactions

L. Romm [a] and G.A. Somorjai [a,b]

[a] *Materials Sciences Division, Lawrence Berkeley Laboratory, Berkeley, CA 94720, USA*
[b] *Department of Chemistry, University of California at Berkeley, Berkeley, CA 94720, USA*

Received 28 October 1999; accepted 15 December 1999

A nozzle, fabricated from nickel, molybdenum, iron, palladium, and quartz was utilized to produce longer chain hydrocarbons, C_mH_n ($m \geqslant 3$, $n \leqslant m$) from C_2 (ethane, acetylene) and C_1 (methane) reactants at nozzle temperature range 1000–1150 °C. The conversion of ethane was close to 100% at $T_{noz} = 1000$ °C, while that of methane reached 20% at $T_{noz} = 1150$ °C. The contact time in the nozzle is in the 10^{-3}–10^{-2} s range. The reactions are first and higher order in reactant pressure. The reaction mechanism involves the formation of free radicals at the nozzle surface followed by gas-phase reactions.

Keywords: methane, ethane, acetylene, benzene, longer chain hydrocarbons, supersonic nozzle beam, contact time, reaction order

1. Introduction

High-temperature, short-contact-time catalytic reactions permit kinetic control of the formation of products by isolation and trapping of reaction intermediates that are thermodynamically less stable under the conditions of the process. Exothermic partial oxidation reactions were carried out in this manner and were the focus of most of the studies. Methanol oxidation to formaldehyde is one important short-contact-time industrial process [1]. Another example is millisecond catalytic partial oxidation of alkanes, which has been extensively studied by Schmidt and co-workers ([2] and references therein).

Recently, Shebaro et al. [3,4] reported the conversion of ethane to benzene in a heated nozzle beam. This is an endothermic reaction, and the high conversion reported points to an interesting reaction mechanism that has not been explored. Upon discussion with one of the authors of these papers (Herschbach) we initiated studies of the high-temperature, short-contact-time conversion of C_2 and C_1 hydrocarbons in an attempt to understand the interesting product distribution and high conversion found for this endothermic reaction.

We have been able to reproduce the results obtained by Shebaro et al. [3,4] using a similar nozzle beam design and obtained high conversion rates of ethane and acetylene to higher hydrocarbons. We have also used other materials to fabricate the nozzle that include iron, palladium, and quartz and found them as active for the coupling reactions of C_2 hydrocarbons as either nickel or molybdenum nozzles [3]. For C_3 and C_4 products the reaction rate is of first order in reactant pressure, while for C_m ($m \geqslant 6$) hydrocarbons formed it is higher than unity. Addition of hydrogen to the reactant mix inhibits the formation of higher hydrocarbon products. Methane can also be converted to higher hydrocarbons under similar reaction conditions.

The reaction mechanism appears to include the generation of free radicals at the nozzle surface and their subsequent gas-phase reactions before exiting the nozzle into the collision-free low-pressure environment in the course of the supersonic expansion.

2. Experimental

The supersonic beam machine specially built for the purposes of the project has three vacuum chambers attached along the axis of the molecular beam. The source chamber is pumped with a 6″ diffusion pump backed with two parallel mechanical pumps. The ultimate pressure is $\sim 1 \times 10^{-7}$ Torr and rises up to 1×10^{-4} when the beam is on. The first differentially pumped chamber is pumped with a 4″ diffusion pump having a LN_2 trap, and the detection chamber is pumped with a 6″ diffusion pump equipped with a LN_2 trap as well. The base pressure in the detection chamber is 5×10^{-10} Torr rising up to 5×10^{-8} Torr at highest beam loads. The detection chamber is equipped with a quadrupole mass spectrometer (QMS, UTI-100) attached at the line of sight of the beam.

The supersonic beam is formed by gas expansion from the high stagnation pressure (up to 1 atm) region into the source vacuum chamber through the nozzle made of catalytic material. We have used Ni, Mo, Fe, Pd and quartz up to date. In the metal case, a button ($\sim$0.8 mm thick) is either welded or crimped to the end of a $1/4''$ in diameter and 7″ long stainless-steel tube, through which a feed gas is supplied to the nozzle. Typical shape of the nozzle is shown in figure 1. The quartz nozzle is fashioned at the end of a

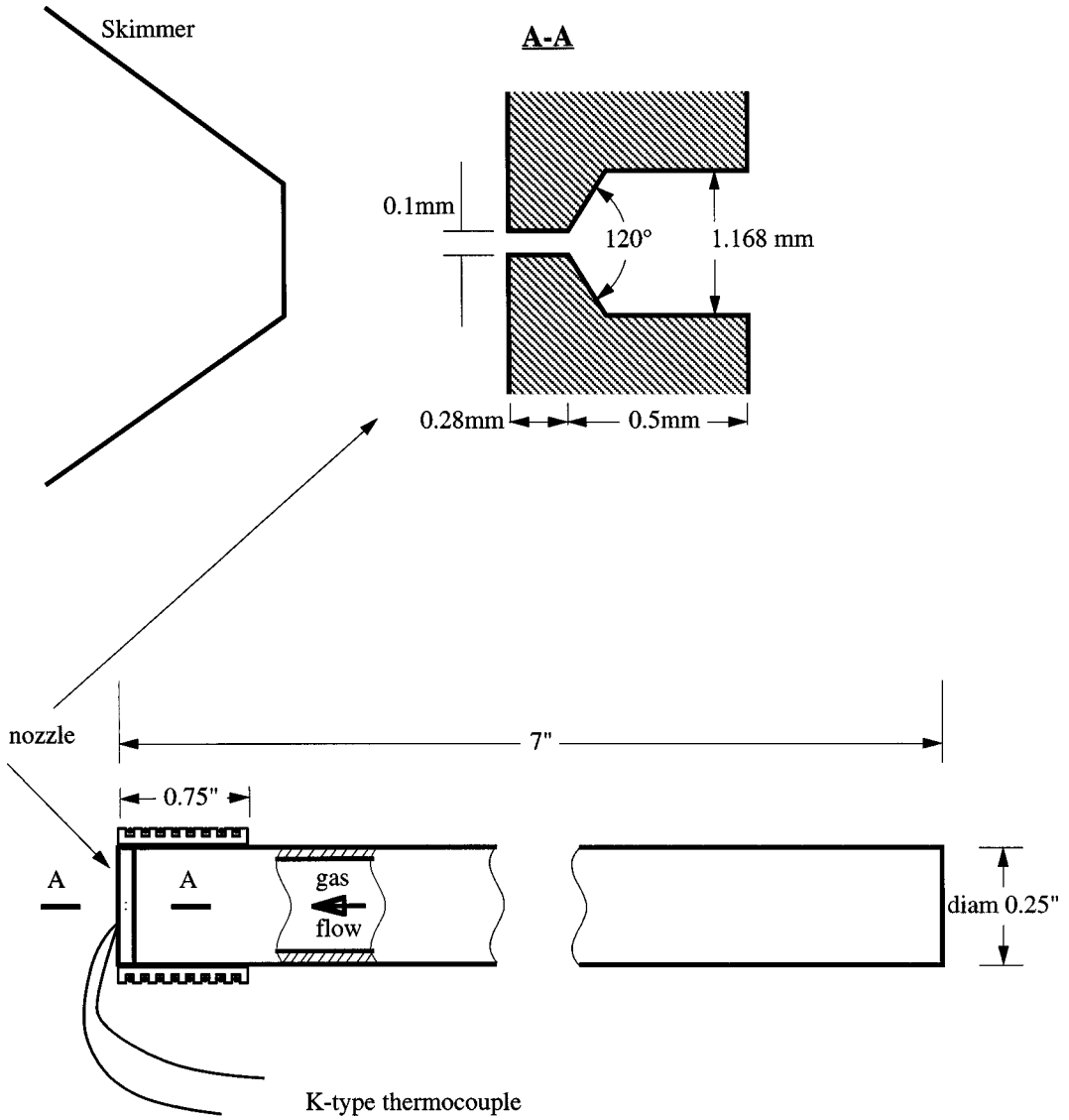

Figure 1. Schematic drawing of the nozzle setup (a case of metal nozzle). The lower picture shows the stainless-steel tube, to which the nozzle button made of catalytic material is welded or crimped. The upper picture presents the cross section of the button with corresponding dimensions and nozzle alignment relative to a skimmer.

quartz tube. The nozzle can be heated to ∼1200 °C. For this purpose, a $3/4''$ long alumina tube is tightly put on the end of the stainless (or quartz) carrier tube (figure 1). There is a groove made in the ceramic tube, and 0.5 mm in diameter Ta heating wire is wound in the groove. The grooved tube is covered with another alumina tube (not shown in figure 1) to shield the heat losses by radiation. A K-type thermocouple is spotwelded (attached in the case of quartz) to the button close to the orifice. The power consumed to heating the nozzle to ∼1000 °C by flowing DC through the heating element is below 200 W. The nozzle is usually cleaned by grinding the orifice with the drill and soaking in acetone [3] prior to its admission to the source chamber. In addition, the nozzle can be cleaned *in situ* by flowing either H_2 or O_2 at different upstream pressures and nozzle temperatures.

In all experiments reported below we used a CW beam. The molecular beam containing the products of the nozzle reactions expands from the nozzle and propagates to the first differentially pumped chamber through a skimmer. The skimmer is made of stainless steel and is a 34 mm long 60° cone with sharp edge orifice of 2.5 mm in diameter. Nozzle-to-skimmer distance is 15–30 mm to ensure the beam collimating from the silence zone [5]. The beam traverses the first differentially pumped chamber, where it can be blocked by a shutter installed on the beam axis. When the shutter is opened the beam enters the detection chamber where it is probed by QMS. The QMS parameters employed are $I_{\text{emis}} = 1.8$ mA, $U_{\text{foc}} = -7.85$ V, $E_{\text{el}} = 70$ V, $E_{\text{ion}} = 15$ V and SEM voltage is 2 kV.

All the mass spectra were recorded and stored on the hard disk using Labview® software. We used ethane (99.9% purity) supplied by Scott Specialty Gases, methane (99.9%) supplied by Matheson, and acetylene (99%) supplied by Boc Gases.

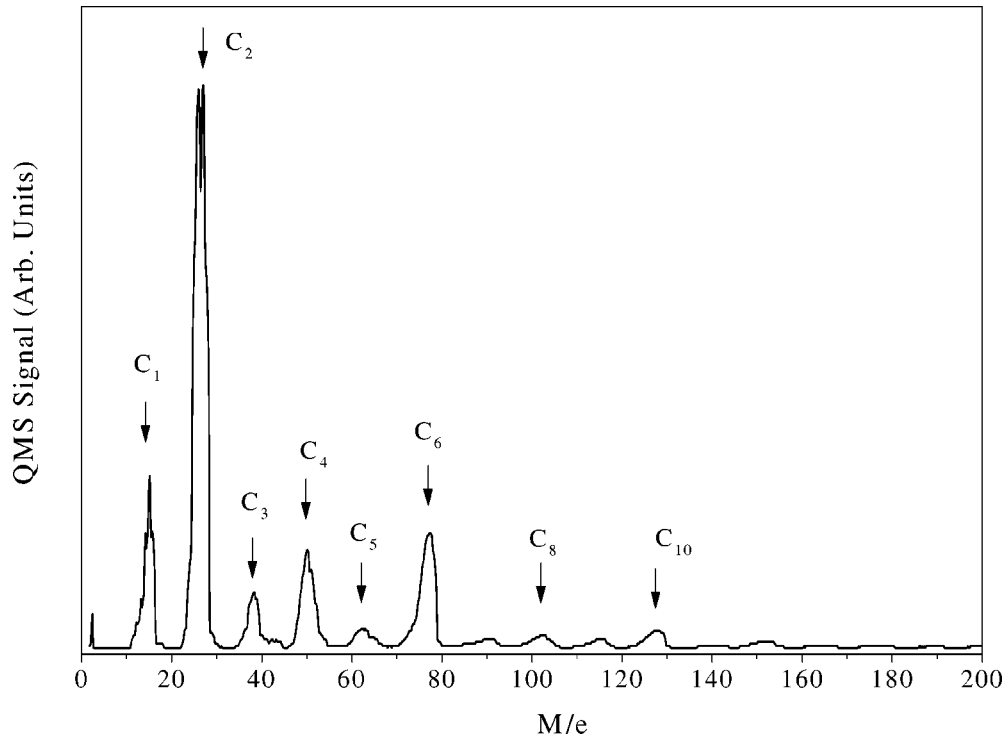

Figure 2. Typical low-resolution mass spectrum of the distribution of various hydrocarbons obtained from ethane flowing through the iron (100 μm in diameter) nozzle at $T_{\text{noz}} = 995\,^{\circ}\text{C}$ and $P_{\text{upstream}} = 671$ Torr. The peaks of the products are marked by the number of carbon atoms they contain.

3. Results

3.1. Ethane conversion

Typical low-resolution mass spectrum is presented in figure 2. It has been obtained by flowing pure ethane through the supersonic nozzle made of iron with diameter of 100 μm (see figure 1). The nozzle temperature was 1000 °C and the upstream stagnation pressure of reactant (ethane) was 671 Torr. The product distribution shown in figure 2 essentially reproduces qualitatively that of Shebaro et al. [3,4] with somewhat lower intensity for heavier hydrocarbons. The differences in product distribution observed may be attributed to the numerous differences in the experimental setup. The intensity distribution of the products varies considerably with the temperature and stagnation pressure (P_{upstream}), however, remains practically unchanged under the same conditions for different nozzle materials. To obtain the product distribution as shown in figure 2, we have had to clean metal nozzles *in situ* prior to the experiments, even though they have been cleaned [3] in air prior to introduction into the vacuum chamber. To flow hydrogen through the metal nozzle at ~500 °C was found to be adequate to have a clean and chemically active nozzle. Oxygen treatment had no effect on the reactivity of the as-introduced nozzle. Thus, we conclude that metal oxides are much less active for the formation of higher hydrocarbons from ethane in the supersonic expansion.

To eliminate a possible effect of the reactivity of the inner surface of the stainless-steel tube heated to high temperatures inside the ceramic heater (see figure 1) we replaced it with 1020 steel. The nickel nozzle (100 μm in diameter) was welded to the tube end, and ethane was used as a reactant. No difference in the product distribution was found compared with using stainless-steel tube.

3.2. Ethane vs. acetylene conversion

As can be seen in figures 2 and 3, the hydrocarbons C_mH_n with $1 \leqslant m \leqslant 21$ are formed upon the supersonic expansion at nozzle temperatures above 1000 °C. It is apparent that the hydrocarbons with even m always exhibit higher intensity than the product molecules with odd number of carbon atoms [3,4]. In addition, dominance of the peak in the high-resolution mass spectrum, referred to the product C_mH_n, where $m = n$ (as shown, for instance, in figure 4 for the C_6 region) infers the C_2H_2 species is to be a building block for higher hydrocarbon formation ($3 \leqslant m \leqslant 6$) in the supersonic expansion. To confirm this, we performed experiments with acetylene as a reactant. Figure 5 shows the product distributions obtained from ethane and acetylene. The intensities of both mass spectra were normalized to mass 26 peaks for comparison. The higher hydrocarbons formed from ethane exhibit somewhat smaller intensity than that from acetylene. A remarkable difference is observed for the C_1 mass region: while ethane decomposition yields considerable amounts of methane among the products, just traces of CH_4 are seen in the case of acetylene as a feed gas. The peaks of masses 12 and 13 on the lower spectrum in figure 5 belong to the cracking patterns of acetylene [6]. The presence of

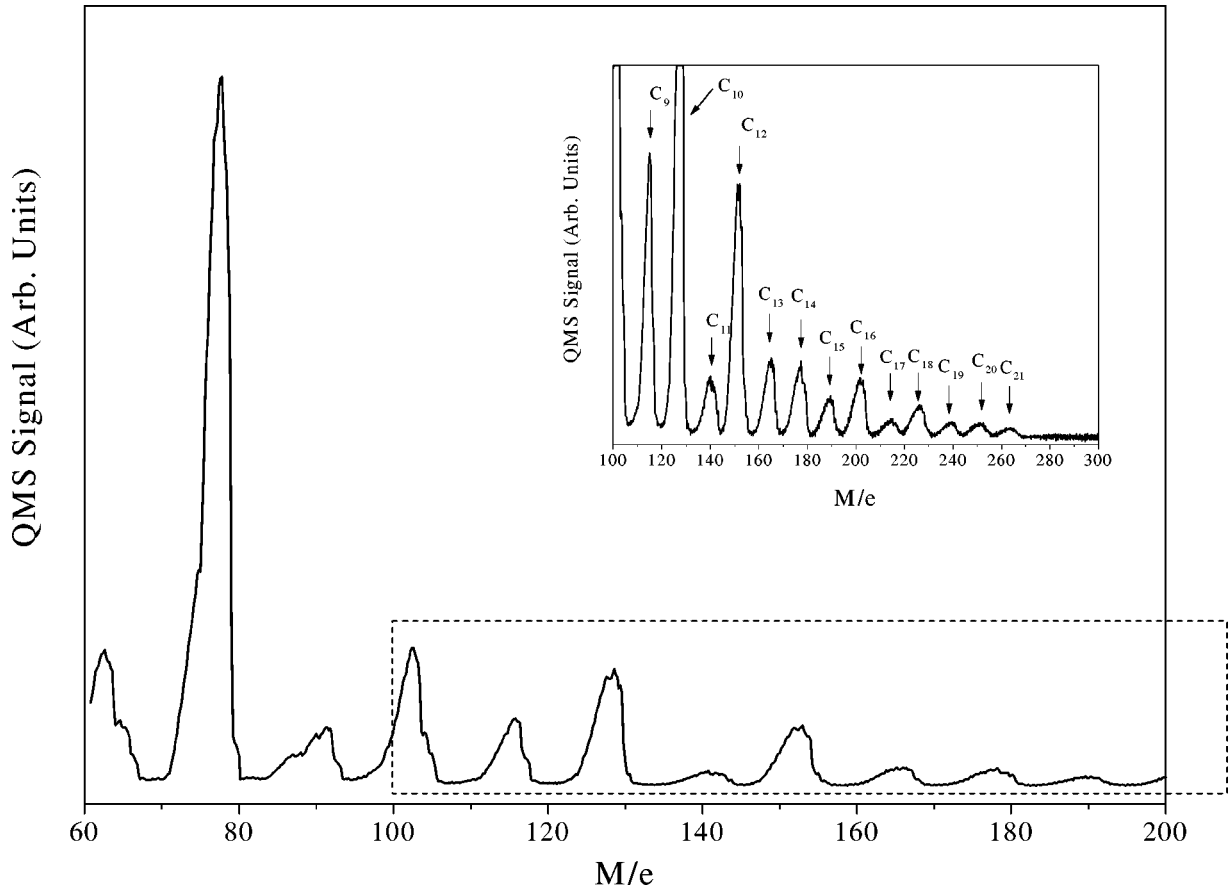

Figure 3. Low-resolution mass spectrum of heavy products formed from ethane in the quartz nozzle (∼200 μm in diameter) at $T_{\mathrm{noz}} \approx 1100\,^{\circ}\mathrm{C}$ and $P_{\mathrm{upstream}} = 165$ Torr. Inset shows tenfold magnification of the mass spectrum for mass-to-charge range between 100 and 300 (dashed rectangle) for the same run. As in figure 2, labels indicate the peaks for the products with the certain number of carbon atoms.

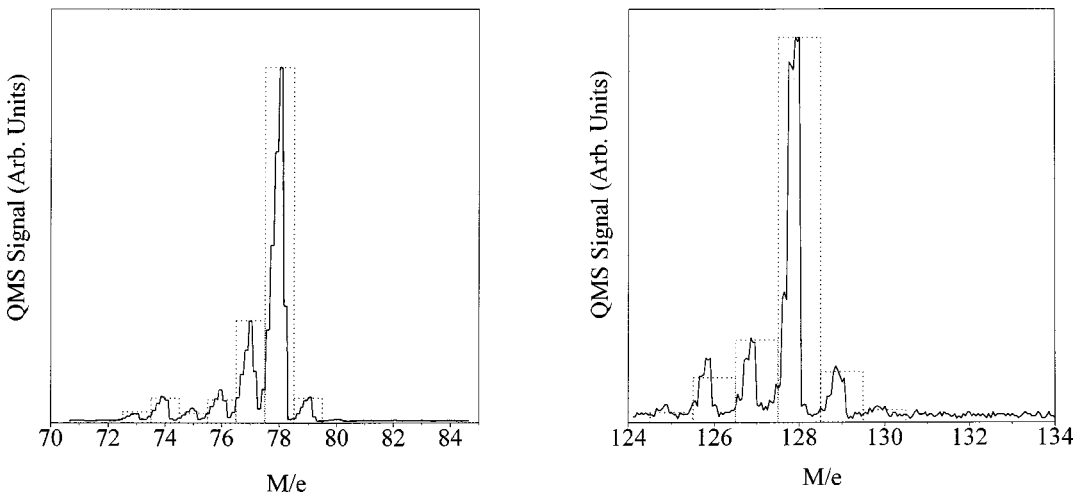

Figure 4. High-resolution mass spectra of C_6H_n (left) and $C_{10}H_n$ mass regions. We can identify the products with reasonable accuracy by comparing the experimentally measured mass spectra with principal fragments of the reference spectra [6] (shown as dotted bargraphs for benzene and naphthalene).

methane in the distribution of products formed in the course of ethane conversion in the supersonic nozzle may be considered as strong evidence of the generation of free radicals. This process is usually thought to be surface-mediated and, thus, catalytic [3,4,7,8].

3.3. Product selectivity and its stagnation pressure dependence

The conversion of ethane at $T_{\mathrm{noz}} \geqslant 1000\,^{\circ}\mathrm{C}$ is almost 100% for all types of materials which were used to fabri-

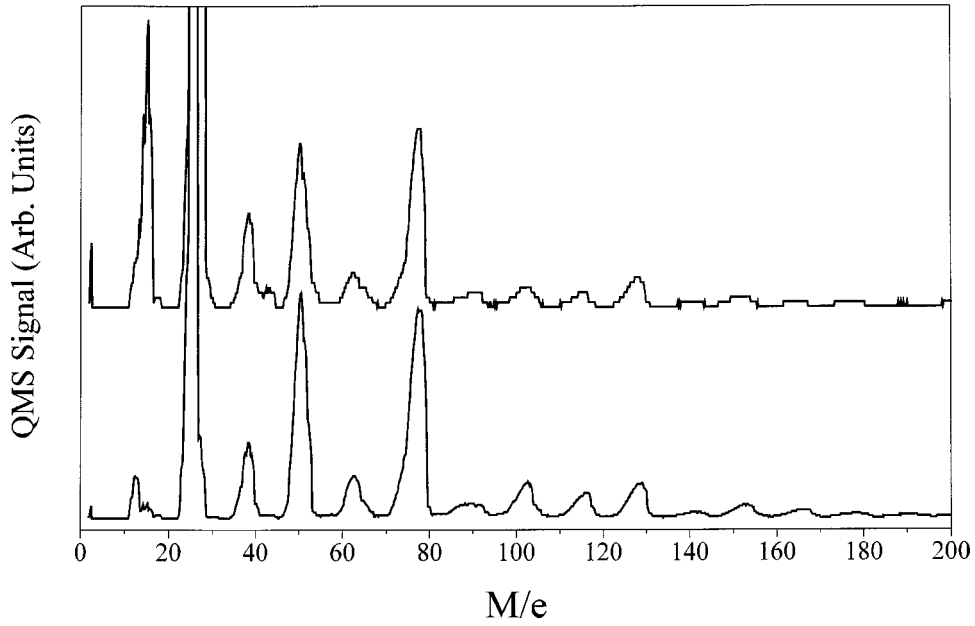

Figure 5. Product distributions obtained for ethane (upper spectrum) as a feed gas for the reaction in the Fe (100 μm diameter) nozzle at $T_{\mathrm{noz}} = 995\,^{\circ}\mathrm{C}$ and for acetylene in Ni (100 μm diameter) nozzle at $T_{\mathrm{noz}} = 900\,^{\circ}\mathrm{C}$. The spectra were normalized to the mass 26 peak. Notice the striking difference of the shown spectra in the C_1 mass region.

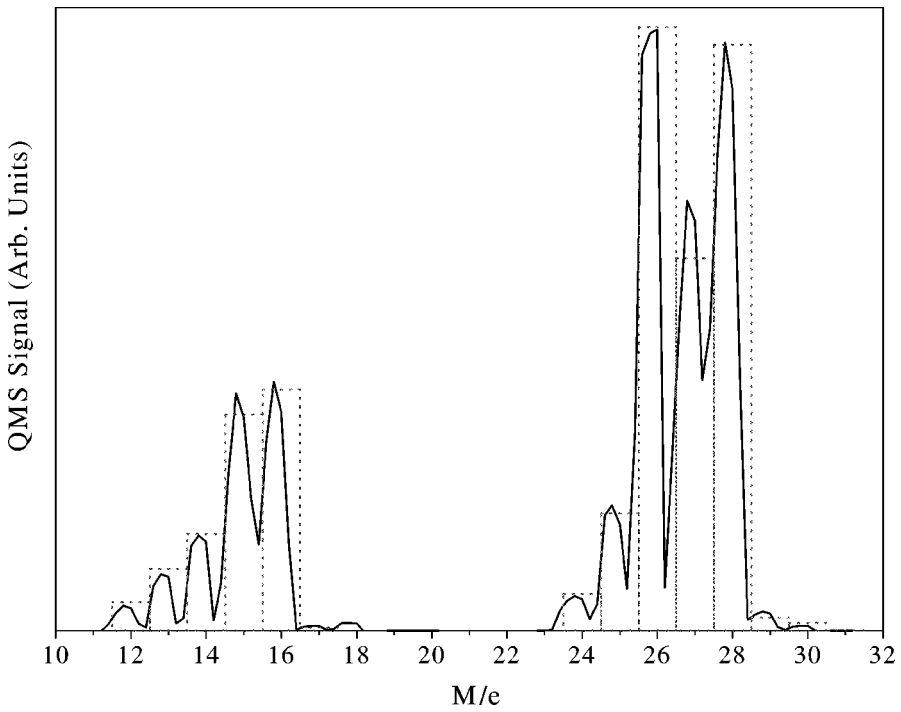

Figure 6. High-resolution mass spectrum of C_1 and C_2 regions for the same nozzle conditions as in figure 2. The dotted bargraph presents a simulated linear combination of intensities of CH_4, C_2H_2, C_2H_4, and C_2H_6. The simulation was done based on zero-order approximation in the quantitative analysis.

cate the supersonic nozzle. Experimental evidence comes from the analysis of the high-resolution mass spectra in the region of 20–32 amu. An example of such a spectrum is given in figure 6. The experimental high-resolution spectrum has been fitted by a simulated linear combination of the intensities of four gases: methane, acetylene, ethylene, and ethane. The simulation in this case has been done using zero-order approximation, which does not allow for variation in ionization efficiencies, multiplier gain, and mass filter transmission among cracking patterns. According to coefficients in the linear combination, only 3% of the reactant ethane remained intact in the process. This number becomes even smaller when a correction on the yield of hydrocarbons higher than C_2H_n is made.

Table 1
Selectivities of some products of the ethane beam reaction in the supersonic nozzle (100 μm in diameter) made of iron and heated up to $1000 \pm 10\,^{\circ}$C.

P_{upstream}	Selectivity							
(Torr)	CH_4	C_2H_2	C_2H_4	C_2H_6	C_3H_3	C_4H_n	C_6H_6	$C_{10}H_8$
152	5.21	20.47	43.23	1.50	3.42	11.30	14.86	0.00
253	5.15	18.00	38.00	1.32	3.60	13.04	18.76	0.00
355	5.27	15.60	33.04	1.20	3.35	13.35	21.47	3.04
519	5.36	12.40	27.90	1.03	3.51	13.45	23.71	7.51
671	5.23	10.54	23.80	0.92	3.47	13.36	26.37	7.88

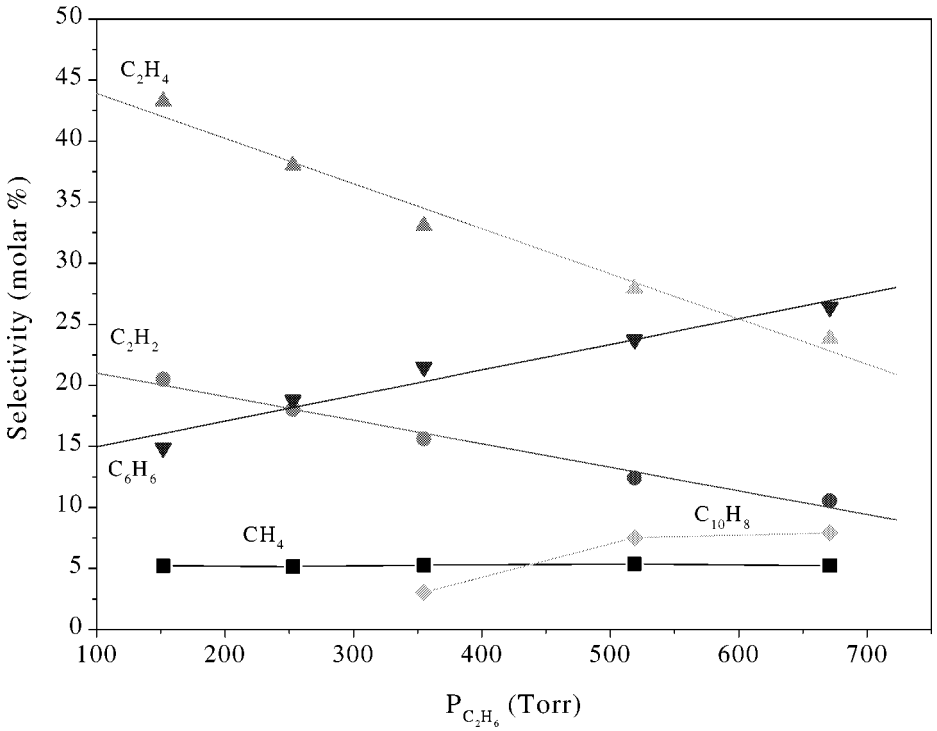

Figure 7. Relative selectivities of some products of ethane beam reaction in the supersonic nozzle (100 μm in diameter) made of iron at $T_{\text{noz}} = 1000 \pm 10\,^{\circ}$C as a function of the stagnation pressures. The products are labeled as follows: methane (■), acetylene (●), ethylene (▲), benzene (▼), naphthalene (♦). The lines for C_2H_2, C_2H_4, and C_6H_6 present a best linear fit of the data, while those for CH_4 and $C_{10}H_8$ are drawn as a guide to the eye.

In fact, since near 100% conversion of ethane is detected, it is important to estimate the selectivity towards certain products among the entire distribution. We have quantitatively analyzed the distribution of intensities of different mass spectra using second-order approximation and drawn the product selectivities. An example of such an analysis is given in table 1 for ethane flowed through the iron nozzle (100 μm in diameter) at the temperature of 1000 °C and various pressures upstream the nozzle. The data in table 1 present the selectivities (in % based on carbon atom balance) of the specific products, which identification is thought to be reasonable (see figure 4, for example). We realize that the data in table 1 carry some systematic error and, hence, may not be considered as absolute selectivities, nevertheless, some useful trends may be noticed. To illustrate this, we plot some of these selectivities in figure 7. The selectivity of benzene increases with the upstream reactant pressure, while that of acetylene and ethylene decreases. These dependencies have a linear character, as it is shown in figure 7. A discernable signal from $C_{10}H_8$ starts to appear only above 350 Torr upstream the nozzle, and the selectivity to this product monotonically grows with stagnation pressure. Note that the relative concentration of methane does not change with P_{upstream}. Nor do the selectivities to C_3H_3 and C_4H_n ($n = 2, 3, 4$) products (see table 1). The comparison of the selectivity vs. P_{upstream} behavior for benzene and methane indicates that the reaction mechanism consists of two major steps. They are generation of free radicals on the surface of the nozzle wall and subsequent bimolecular reactions in the gas phase between molecules and these desorbing radicals, swept from the surface in the course of beam expansion.

3.4. Deactivation of nozzle

The lifetime of a supersonic nozzle strongly depends upon its temperature. With ethane flowing through metal nozzles at 1000 °C, we have been able to carry out exper-

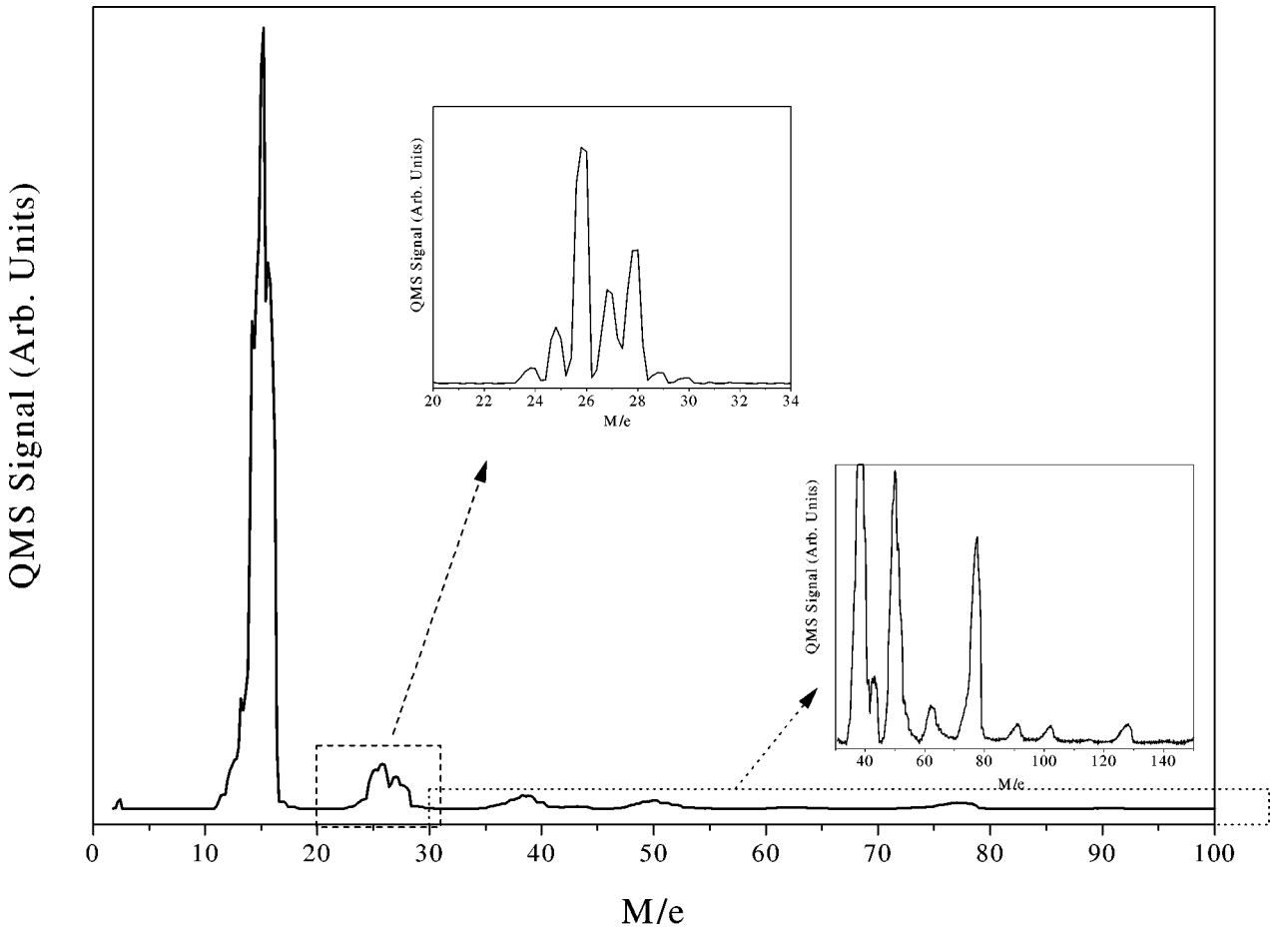

Figure 8. Product distribution (low resolution) from methane beam flowed through the quartz nozzle (200 μm in diameter) at $T_{\text{noz}} \approx 1150\,^{\circ}\text{C}$ and $P_{\text{upstream}} = 90$ Torr. On the upper inset the high-resolution mass spectrum of the C_2 region is shown. The C_2H_2/C_2H_4 ratio is estimated to be equal to approximately 1 : 1. Lower onset presents the low-resolution mass spectrum of the 30–150 amu region for this run, taken at 100 times higher sensitivity. A shoulder at mass 44 belongs to CO_2 from ambient gas.

iments for up to 10 h, until considerable deactivation of the nozzle occurred. This deactivation is caused by coke formation in the heating zone behind the nozzle orifice and consecutive clogging of the nozzle. It has been checked visually that the nozzle capillary remains clean in the course of reaction even though a large amount of coke is produced. In some cases we were able to clean the nozzle by burning the coke in oxygen *in situ*. In other cases we had to take the nozzle out of the source chamber and clean it as described in section 2. The friendliest material in the sense of coke burning is quartz. We have never taken the quartz nozzle outside the vacuum chamber for the purpose of cleaning.

3.5. Methane conversion

We report in the present letter the formation of higher hydrocarbons from methane in the nozzle made of quartz. We carried out the experiments under severe conditions of $T_{\text{noz}} \approx 1150\,^{\circ}\text{C}$ and measured the distribution of products similar to that in the case of ethane taken as a reactant (see figure 8). We had to maintain low upstream pressure (90 Torr) in order to avoid rapid coke formation in the heating zone. As can be estimated from the intensities, the yield of higher hydrocarbons is much lower than in the case of ethane beam. The conversion of methane was about 20%, based on the balance of carbon atoms. In the product distribution, the intensity decreases with number of carbon atoms in the product molecule in contrast to the case of ethane beam, where the intensity of C_3H_3 is lower than either C_4H_n or C_6H_6 (compare with figures 2 and 5). The yield of acetylene, C_3H_3, C_4H_n, and benzene was about 4% each.

We checked and ruled out the upstream pressure difference as a reason for this discrepancy. For this purpose, we flowed ethane at $P_{\text{upstream}} = 80$ Torr through the nickel nozzle, although, at $T_{\text{noz}} = 1000\,^{\circ}\text{C}$. The product distribution obtained reproduces that presented in figure 2. No reaction products were detected in the methane beam flowed through the metal nozzle at highest temperatures (about 1150 °C), at which the nozzle does not clog for a few minutes.

4. Discussion

The conversion rate of ethane to higher hydrocarbons during the supersonic expansion at the nozzle temperature of 1000 °C was measured to be too high to meet require-

ments of thermodynamics equilibrium. In fact, thermodynamics predict, that ethane would decompose predominantly to carbon on the surface and hydrogen in the gas phase in the absence of gas flow. We made an attempt to estimate the turnover number for benzene and found it to be not less than ten benzene molecules per metal atom per second for $T_{\mathrm{noz}} = 1000\,^{\circ}\mathrm{C}$ and $P_{\mathrm{upstream}} = 671$ Torr, provided the beam flux is greater than 1×10^{17} molecules $\mathrm{cm}^{-2}\,\mathrm{s}^{-1}$ [9]; the selectivity to benzene is ~20%, diameter of nozzle orifice is 100 μm, typical atomic density of (111) surface plane is $\sim 1.5 \times 10^{15}$ atoms cm^{-2}, and assuming that the benzene molecules are formed only inside the nozzle capillary. The last assumption seems to be plausible since oxidized metal nozzles are found to be nonreactive relative to the formation of higher hydrocarbons. Practically all metal nozzles exhibited much lower rate of conversion of ethane to higher hydrocarbons when used as introduced. Hydrogen treatment of the nozzles, however, followed by the experiment, enhanced the signals of the heavy hydrocarbons up to ten times. In addition, the high-resolution C_2 region of the mass spectra showed a strong signal from unreacted ethane and practically no signals from acetylene and methane prior to the hydrogen treatment of the nozzle. The conversion of ethane reached ~100% following the cleaning of the nozzle in hydrogen. The *in situ* oxidation of the nozzle somewhat inhibits its reactivity, however, no systematic study has been carried out as yet of oxygen-induced nozzle deactivation.

The mechanism of chemical reactions, in which hydrocarbon molecules participate in this temperature regime, is usually discussed in terms of free radical formation and reaction [8]. Our goal is to gain an insight into the mechanism of free radical formation and the role of the nozzle surface, and try to control reaction pathways to redistribute the products toward desirable selectivities. The presence of free radicals may be accounted for on the basis of the following arguments. Formation of methane among the products should be solely due to ethane cracking $C_2H_6 \rightarrow 2CH_3^{\bullet}$ (C–C bond strength in ethane is ~83.2 kcal mol^{-1}) on the hot nozzle wall, and subsequent hydrogenation of methyl to methane on the surface followed by desorption of the molecule to the gas phase. Under similar conditions acetylene does not crack due to its much stronger C≡C triple bond (figure 5). The reaction pathway requires either H or H_2 species to be present. Formation of H can easily proceed through hydrogen atom abstraction [7] $C_2H_6 \rightarrow C_2H_5^{\bullet} + H$ (C–H bond strength in ethane is ~89 kcal mol^{-1}). Thus, the ethane cracking and H atom abstraction may be viewed as chain initiation reactions.

Alternatively, methyl radicals may induce metathetical [10] reaction $CH_3^{\bullet} + C_2H_6 \rightarrow CH_4 + C_2H_5^{\bullet}$. This reaction is exothermic and, hence, may be considered as a chain propagation reaction. The C–H bond in ethane is weaker than that in methane (~98.5 kcal mol^{-1}), hence the hydrogen atom abstraction from methane is unlikely under the reaction conditions. Once ethyl radicals are formed, further reactions may occur, such as $C_2H_5^{\bullet} \rightarrow C_2H_4 + H$ and $2C_2H_5^{\bullet} \rightarrow C_2H_4 + C_2H_6$. Ethylene is further dehydrogenated to produce acetylene and, subsequently, higher hydrocarbons by coupling. Comparison of the selectivity vs. P_{upstream} dependencies (figure 7 and table 1) between methane and benzene infers that formation of benzene and, possibly, heavier hydrocarbons, which are quite stable and, hence, appear in the supersonic beam, is higher than first-order reaction, thus, occurring in the gas phase prior to or during the expansion. The relative concentrations of CH_4, C_3H_3, and C_4H_n molecules remain constant; their signals in the mass spectra increase linearly with the stagnation pressure. The increase of the benzene intensity as a function of the upstream pressure was measured to be faster than linear, thus, indicating that the reaction order of the benzene formation is probably higher than unity.

The suggestion that the formation of higher hydrocarbons through consecutive coupling of C_2H_2 species is supported by the dominance of the products in the mass spectra with even number of carbon atoms. Similarity of the product distributions from ethane and acetylene beams (excluding the C_1 mass region) confirms this statement. The presence of molecules with odd number of carbon atoms in both product distributions (figure 5), thus, may be accounted for by cracking rather than by coupling the methyl radical.

Once the free radicals are formed on the surface and desorb to the gas phase, the reactions may follow numerous channels. However, thermodynamically these channels would lead to the ultimate decomposition to carbon and hydrogen, as it was mentioned above. So, our ability to observe various hydrocarbons is solely due to the effect of supersonic expansion [3,4] that provides kinetic control of the reaction. This technique makes possible to terminate the reaction by rapid withdrawal of the intermediate products into a collisionless environment. The key parameter in this process is the very short contact time between the product molecules and hot nozzle walls. The contact time is estimated to be of the order of 1–10 ms [3]. Even free radicals can be observed in the product distribution due to this short contact time. Thorough analysis of the C_3 mass region in the spectrum of products shows [3,4] that the mass 39 peak (the principal one in C_3 series) likely belongs to the C_3H_3 propargyl radical.

The supersonic expansion technique opens many opportunities to control hydrocarbon conversion towards desired products at very high turnover rates and selectivities. For example, mixing reactants and adjusting their partial pressures in the mixture can be employed to obtain desirable products with considerable yields. No expensive catalysts would be needed for these purposes. For example, we were able to greatly suppress the formation of higher hydrocarbons by mixing hydrogen with ethane [11] and observed formation of more ethylene [12] and acetylene instead.

5. Summary

The conversion of ethane in the supersonic nozzle (made of Ni, Mo, Pd, Fe, or quartz) beam reactions is close to

100% at $T_{\text{noz}} \approx 1000\,^{\circ}\text{C}$. The yield of longer chain hydrocarbons C_mH_n, where $m \geqslant 3$, $n \leqslant m$, depends on the stagnation pressure and reaches ∼60% at the maximum pressure applied. The conversion of methane is about 20% at $T_{\text{noz}} \approx 1150\,^{\circ}\text{C}$ for the nozzle made of quartz.

The proposed mechanism consists of two major steps, which include the generation of free radicals on the hot nozzle surface followed by their rapid desorption into the gas phase and subsequent consecutive bimolecular reactions. The supersonic expansion makes the kinetic control of the formation of longer chain hydrocarbons possible due to short gas–surface contact time and withdrawal of intermediate products from the hot reaction space into a collisionless environment.

Acknowledgement

We gratefully acknowledge L. Shebaro and D. Herschbach for fruitful and stimulating discussions and inputs. We have benefited from helpful contribution from S.H. Kim and Y. Borodko. This work was supported by the Director, Office of Energy Research, Office of Science, Division of Materials Sciences, of the US Department of Energy under Contract No. DE-AC03-76SF00098.

References

[1] C.N. Satterfield, *Heterogeneous Catalysis in Industrial Practice*, 2nd Ed. (McGraw-Hill, New York, 1991) ch. 8.
[2] D.A. Goetsch and L.D. Schmidt, Science 271 (1996) 1560;
A.S. Bodke, D.A. Olschki, L.D. Schmidt and E. Ranzi, Science 285 (1999) 712.
[3] L. Shebaro, B. Abbott, T. Hong, A. Slenczka, B. Friedrich and D. Herschbach, CPL 271 (1997) 73.
[4] L. Shebaro, S.R. Bhalotra and D. Herschbach, J. Phys. Chem. A 101 (1997) 6775.
[5] D.R. Miller, in: *Atomic and Molecular Beam Methods*, Vol. 1, ed. G. Scoles (Oxford Univ. Press, Oxford, 1988) ch. 2.
[6] NIST Chemistry Web Book, NIST Standard Reference Database Number 69, November 1998 release. See http://webbook.nist.gov/chemistry/.
[7] D.J. Driscoll and J.H. Lunsford, J. Phys. Chem. 89 (1989) 4415.
[8] G.A. Olah and Á. Molnár, *Hydrocarbon Chemistry* (Wiley, New York, 1995).
[9] J.B. Anderson, R.P. Andres, J.B. Fenn and G. Maise, in: *Rarefied Gas Dynamics*, Supplement 3, Vol. 2, ed. J.H. de Leeuw (Academic Press, New York, 1966) p. 106.
[10] J.A. Kerr and S.J. Moss, *Handbook of Bimolecular and Termolecular Gas Reaction* (CRC Press, Boca Raton, FL).
[11] L. Romm and G.A. Somorjai, to be published.
[12] L. Kneil, O. Winter and K. Stork, *Ethylene, Keystone to the Petrochemical Industry* (Dekker, New York, 1980).